Design, Prototyping and Measurement of EVLA Ku-Band Feed Horn

Sivasankaran Srikanth
NRAO
November 4, 2009

Abstract:

A prototype of the Ku-band (12-18 GHz) feed horn for the EVLA has been designed, built and tested. This feed horn is a corrugated horn with a linear taper of 10.38˚; has an aperture diameter of 15.6 λ and a length of 42.3 λ at the center frequency. The horn has five machined aluminum sections including the circular input waveguide section. The feed horn has an average illumination taper of -14.0 dB at the edge of subreflector in the 12-18 GHz range. Cross-polarization is less than -27 dB in the design band. Measured return loss is better than 30 dB.

Introduction:

For a receiver temperature of 21 K, a feed illumination taper of -13 to -14 dB at the edge of the subreflector (9.3º half-angle) resulted in maximum gain/system temperature (G/T) at 15 GHz for the EVLA antenna. In order to obtain a -13.5 dB taper with a 1.5:1 bandwidth ratio, a linear taper horn would require an aperture of diameter of 12.3". This feed horn would easily fit in the assigned area. A linear taper horn with ring-loaded corrugations in the mode converter was chosen for the Ku-band. This memo covers the design of the feed horn; prototype construction and details of measurements done at the Outside Antenna Test Range (OATR) in Socorro and at the Outside Antenna Range (OAR) in Green Bank. Far-field range measurements on two horns and comparisons with theory are shown. Results of return loss measurements are also shown.

Design and Prototyping:

The semi flare angle θ_0 of prime-focus feed horns are usually large (>30˚) while for secondary focus systems the feed horns have narrow flare angles. The spherical phase error Δ at the aperture of a narrow flare angle horn is given by

$$\Delta = \frac{r_1 * \tan\left(\frac{\theta_0}{2}\right)}{\lambda}$$

Here r_1/λ is the aperture radius in wavelengths. The beamwidth of horns with $\Delta<0.4$ depends on the aperture size r_1/λ and hence is frequency dependent. Such horns are termed "narrow band" horns. For $\Delta>0.5$ the beamwidth is mainly determined by θ_0, the phase center of the horn is near the throat and remains almost fixed with respect to frequency. These horns are termed "wide-band" horns. For the Ku-band horn, a value of 0.58 is chosen for Δ at the lowest frequency of operation. A combination of θ_0=10.38˚ and aperture diameter of 12.3" gives the specified feed taper of -13.5 dB at the edge of the subreflector of the EVLA antenna.

The circular waveguide at the input end of the feed has a diameter of 0.7795". The mode converter has six ring-loaded corrugations with constant depth and has a linear taper of 8˚. The first corrugation starts at a diameter of 0.798" that prevents the generation of the EH_{12} mode. A cosine taper of length 1.475" connects the input end of the feed with the mode converter. The number of corrugations is 4 per wavelength at 18 GHz. The pitch of the corrugations is 0.164" and the width is 0.112". A smooth transition over a length of six pitches provides the change in taper from 8˚ at the output of the mode

converter to the taper of 10.38˚ of the feed horn. There are 187 corrugations past the mode converter and the depth changes from about 0.42λ (at 18 GHz) at the output of the mode converter to 0.28λ at the aperture of the horn.

The fabricated feed horn has five sections. The first section has the input circular waveguide and the housing for the ring-loaded corrugations. Machined aluminum disks that make up the ring-loaded corrugations are press fitted into this housing. The main body of the feed horn is in sections 2 through 5 and these are machined from aluminum castings. Figure 1 shows the general arrangement of the Ku-band feed horn. The length of the feed horn is 33.3".

Range Measurement:

Feed horn #01 was measured at the OATR in Socorro between June 10 through 13, 2008. A circular (0.7795" diameter) to rectangular (0.311" x 0.622") transition fabricated using EDM (electric discharge machining) technique was used in the measurements. The horn was mounted on a Styrofoam cradle and an interface wooden frame was used to install the feed on the 12-foot foam tower (Figure 2a). The center of rotation was set at a distance of 27" behind the aperture of the feed. Two source horns, Pasternack PE9854-20 and Antenna Research Associates (ARA) MWH1218A were used. Patterns presented here were measured with the ARA standard gain horn. The transmit horn aperture was about 26" in front of the transmit tower. The measurement distance was 26.375', which is greater than $2D^2/\lambda$ at 12 GHz. At higher frequencies the measurement distance is between D^2/λ and $2D^2/\lambda$. The angular range of measurement was set to ±90º and data was recorded at 0.2° intervals. The frequency range was set to 12-18 GHz with 0.2 GHz intervals. Patterns were measured in the E-, H-, and 45º-planes.

Measured amplitude and phase patterns at 15 GHz in the E-plane are shown in Figure 3. Theoretical amplitude pattern (pink) is overlaid on the measured pattern in Figure 3a, showing good agreement down to the -25 dB level. Patterns in the H-plane at 15 GHz are shown in Figure 4. The match between theory and measurement is good down to -35 dB. The noise floor of the measured pattern in the E-plane is at approximately -32 dB, while in the H-plan, the noise floor is at -40 dB. At 18 GHz, the noise floor is at -25 dB in the E-plane and at -32 dB in the H-plane. The feed mounting frame and the cradle had very limited freedom of movement on the tower and as a result symmetry of the phase pattern could not be achieved (Figures 3b & 4b). In the 45º-plane, co-polarized and cross-polarized patterns were measured. Figure 5 shows the measured cross-polarization from 12-18 GHz. The sidelobes are below -23 dB for frequencies below 17GHz. The level of -10dB at 18 GHz is an artifact of the non-orthogonality between the antenna under test (AUT) and the source feed and low signal levels.

A production feed horn was measured at the OAR in Green Bank (Figure 2b) between August 4 through 6, 2009. At this range the AUT is mounted on a box that can be translated in both the longitudinal and transverse directions. The axis of the AUT is at a height of 31.5' above the ground and the distance between the source horn and the AUT was 51'. A Scientific Atlanta SA Model 12-12 standard gain horn (12.4-18 GHz) was used as the source horn. This antenna range allows measurement at only one frequency at a time. Measurements were made from 12-18 GHz at 1 GHz intervals in the E-, H-, and 45˚-planes. Measurements were carried out at 11.5 and 18.5 GHz as well. The azimuth range was set at ±60 ˚ and data recorded at 1˚ intervals. At first, phase was measured in the ±30˚ range for different axial positions of the AUT in order to locate the phase center at each frequency. The axial position that produces the flattest phase response in the ±10˚ range was noted and the corresponding distance of the aperture of the feed horn from the center of rotation gives the phase center distance. This axial position of the horn was used at each frequency while recording the amplitude and phase patterns.

Figures 6, 7, and 8 show the measured patterns overlaid on simulated patterns in the E-plane. At 12 and 15 GHz, the agreement between the two patterns is good down to -35 dB. At 18 GHz, the measured pattern is narrower; however, the match between the patterns is good down to -13 dB. Measured and theoretical patterns in the H-plane are shown in Figures 9, 10, and 11. The agreement between the two patterns is good down to -40 dB at 12 and 15 GHz. Figures 12, 13, and 14 show the measured E- and H-plane patterns superimposed. There is excellent agreement between the two patterns showing good circular symmetry of the beam over the 12-18 GHz range. Amplitude patterns in the E-plane over the 11.5-18.5 GHz range are shown in Figure 15 and phase patterns are shown in Figure 16. The symmetry of the phase patterns was achieved because of the availability of transverse translation on the Green Bank OAR. Amplitude and phase patterns in the H-plane are shown in Figures 17 and 18, respectively. The illumination tapers at the edge of the subreflector at different frequencies are shown in Table 1. The phase center locations from the aperture of the feed horn as a function of frequency are shown in Table 2.

Co-polarized and cross-polarized patterns were measured in the 45°-plane. After the co-polarization measurement, with the AUT positioned on boresight, the source horn was rotated about its axis by 90° and fine adjustments were made about this angle to obtain a signal null. With this position of the source horn, pattern recorded gives the cross-polarization of the feed horn. Cross-polarized patterns are shown in Figure 19. The peak of the cross-polarization (with respect to the peak of co-polarization) stays below -30 db except at 15 GHz where the peak is at -27.3 dB. Return loss measurements were carried out on two Ku-band feed horns. Two shorts of lengths ⅛ and ⅜ of guide wavelength at 15 GHz and a sliding load were used to calibrate the vector network analyzer. The measured results between 11.5 GHz and 18.5 GHz, for the two horns are shown along with theoretical predictions in Figure 20. Within the operating band, the return loss for both feeds is below 30 dB.

Conclusion:

The Ku-band feed horn has an average illumination taper of -14 dB at the edge of the subreflector over the 12-18 GHz range. Measured patterns agree well with theory down to the -35 dB level. The input match is excellent and cross-polarization of the feed horn is better than -27dB. The distance of phase center of the feed horn from the aperture varies between 26.4" at 12 GHz and 31.5" at 18 GHz. J. Ruff was responsible for mechanical design of the feed horn. The machine shops at the VLA and Green Bank carried out the machining of the horns. The assistance provided by D. Mertely, H. Dinwiddie, C. Dunlap, C. Frentzel, D. Monroy, M. Lopez and J. Scarbrough at Socorro and G. Anderson and J. Bauserman in Green Bank in the range measurements is appreciated.

Table 1. Illumination taper at the edge of the subreflector (9.3 ˚)

Frequency (GHz)	12	13	14	15	16	17	18
E-plane (dB)	-13.68	-13.07	-13.13	-14.20	-14.58	-14.85	-13.81
H-plane (dB)	-12.91	-13.44	-14.37	-12.71	-14.12	-15.94	-15.51

Table 2. Distance of Phase Center from aperture

Frequency (GHz)	12	13	14	15	16	17	18
E-plane (")	25.86	26.89	27.91	28.96	29.75	30.62	31.49
H-plane (")	26.90	27.59	28.26	28.94	29.74	30.63	31.49

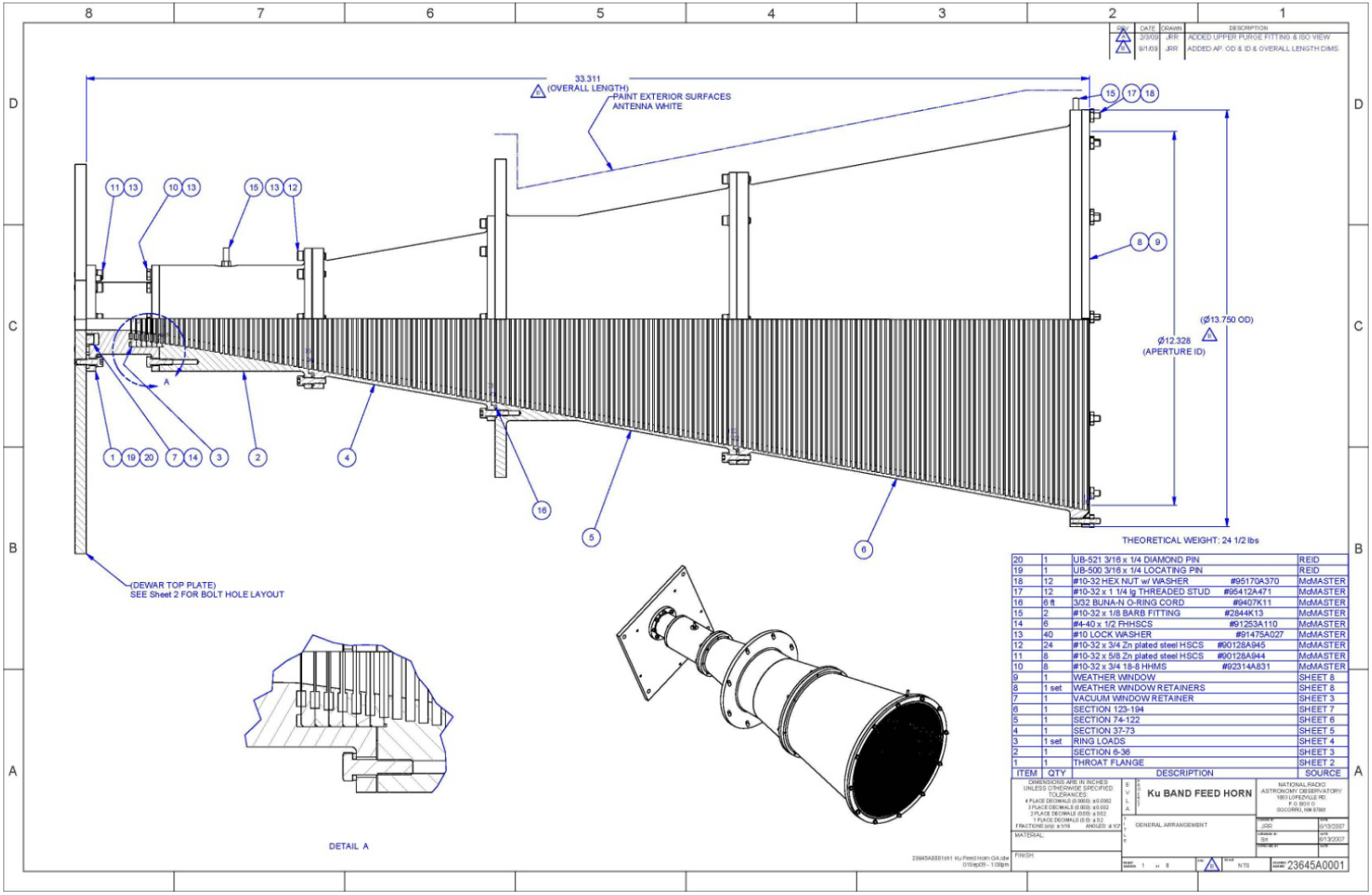

ITEM	QTY	DESCRIPTION	SOURCE
20	1	UB-521 3/16 x 1/4 DIAMOND PIN	REID
19	1	UB-500 3/16 x 1/4 LOCATING PIN	REID
18	12	#10-32 HEX NUT w/ WASHER #95170A370	McMASTER
17	12	#10-32 x 1 1/4 lg THREADED STUD #95412A471	McMASTER
16	6 ft	3/32 BUNA-N O-RING CORD #9407K11	McMASTER
15	2	#10-32 x 1/8 BARB FITTING #2844K13	McMASTER
14	6	#4-40 x 1/2 FHHSCS #91253A110	McMASTER
13	40	#10 LOCK WASHER #91475A027	McMASTER
12	24	#10-32 x 3/4 Zn plated steel HSCS #90128A945	McMASTER
11	8	#10-32 x 5/8 Zn plated steel HSCS #90128A944	McMASTER
10	8	#10-32 x 3/4 18-8 HHMS #92314A831	McMASTER
9	1	WEATHER WINDOW	SHEET 8
8	1 set	WEATHER WINDOW RETAINERS	SHEET 8
7	1	VACUUM WINDOW RETAINER	SHEET 3
6	1	SECTION 123-194	SHEET 7
5	1	SECTION 74-122	SHEET 6
4	1	SECTION 37-73	SHEET 5
3	1 set	RING LOADS	SHEET 4
2	1	SECTION 6-36	SHEET 3
1	1	THROAT FLANGE	SHEET 2

Figure 1. General arrangement of Ku-band Feed Horn

Figure 2a. Feed Horn at the Socorro OATR

Figure 2b. Feed Horn at the Green Bank OAR

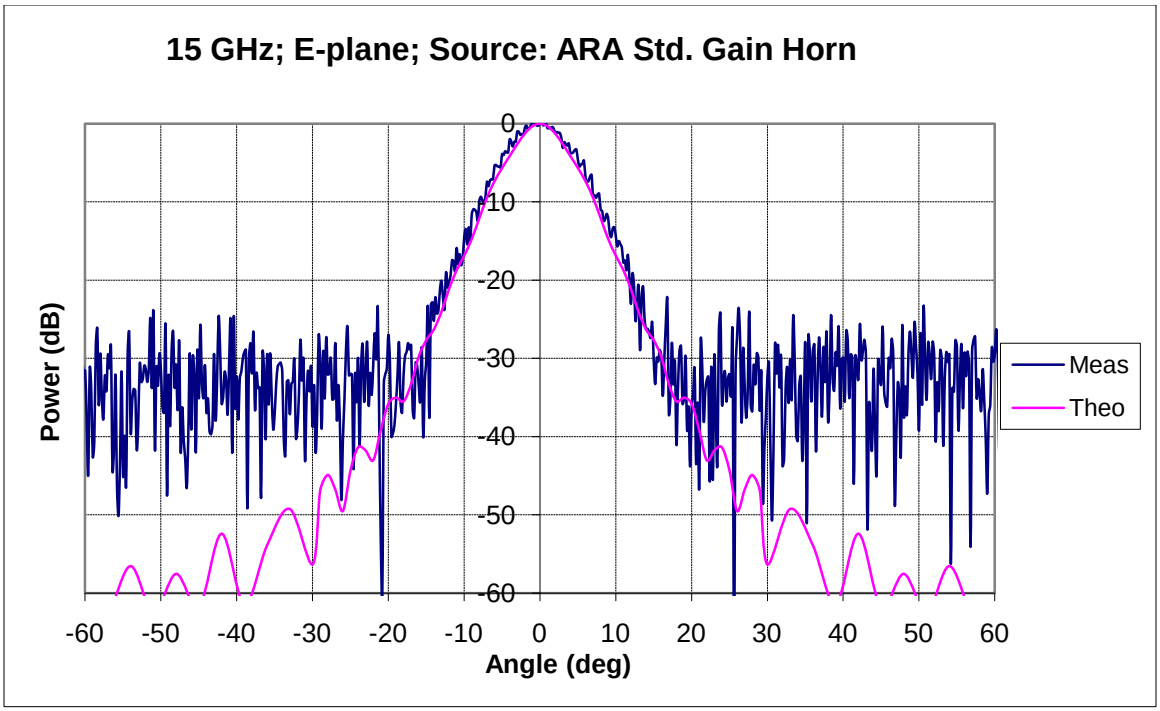

Figure 3a. Measured (OATR) and Theoretical Patterns at 15 GHz; E-plane

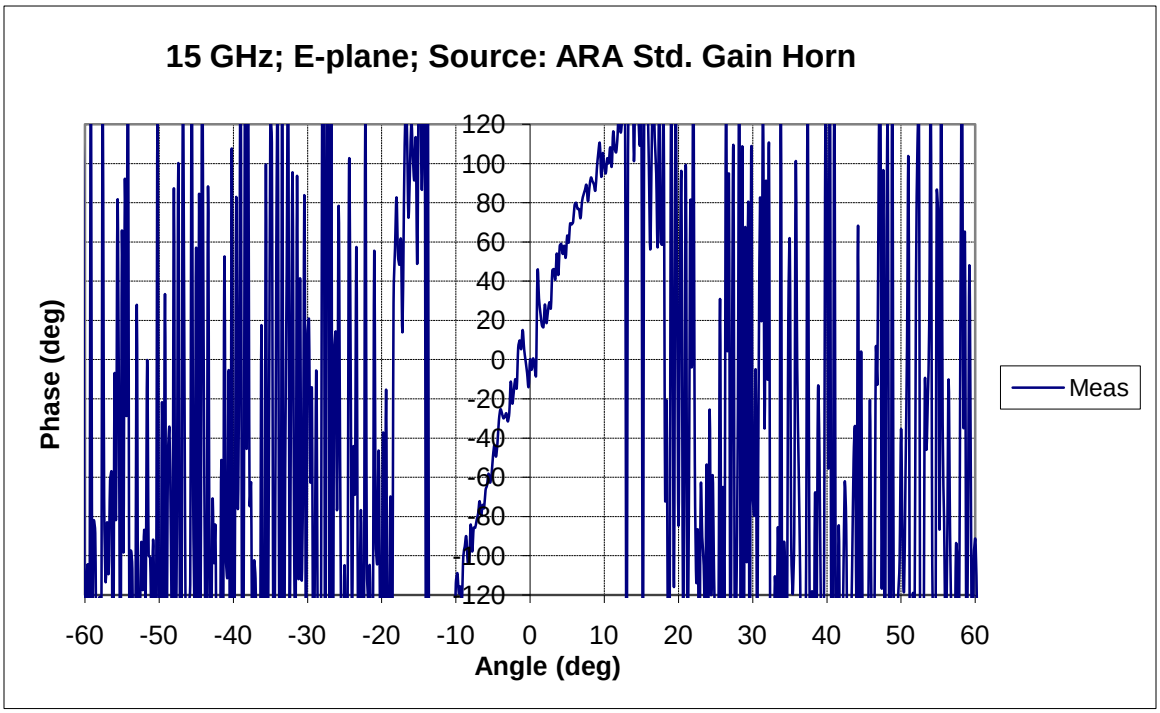

Figure 3b. Measured (OATR) Phase Pattern at 15 GHz; E-plane

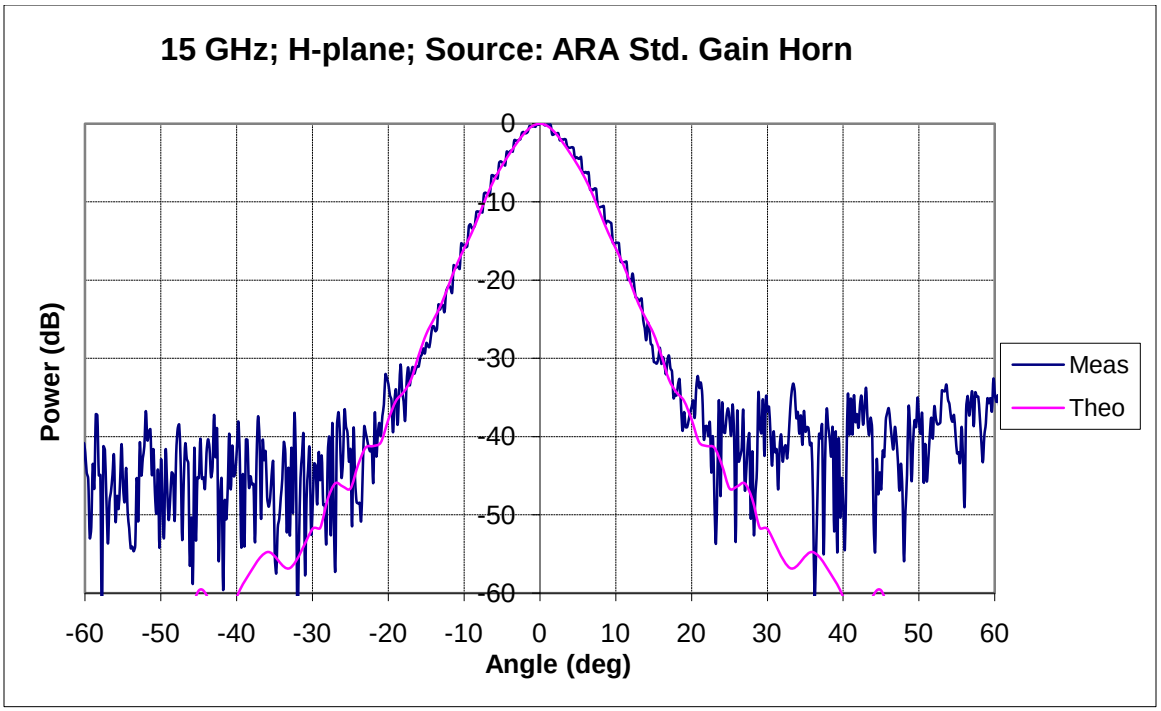

Figure 4a. Measured (OATR) and Theoretical Patterns at 15 GHz; H-plane

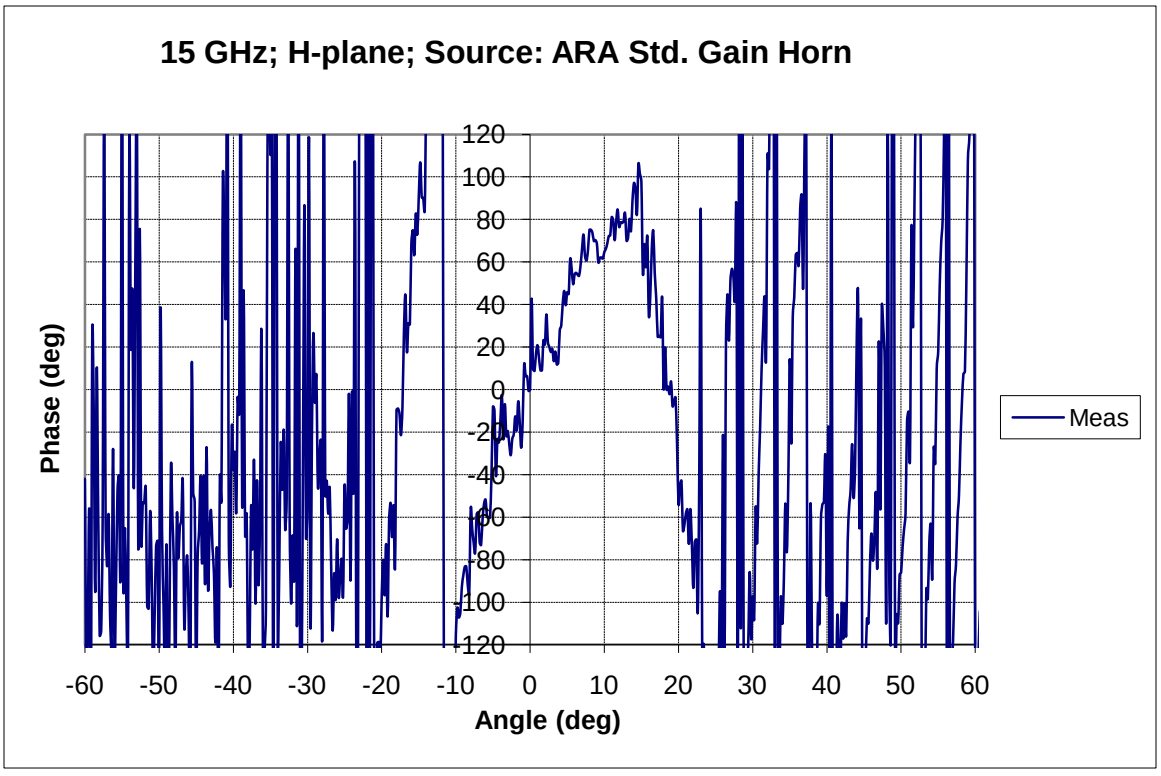

Figure 4b. Measured (OATR) Phase Pattern at 15 GHz; H-plane

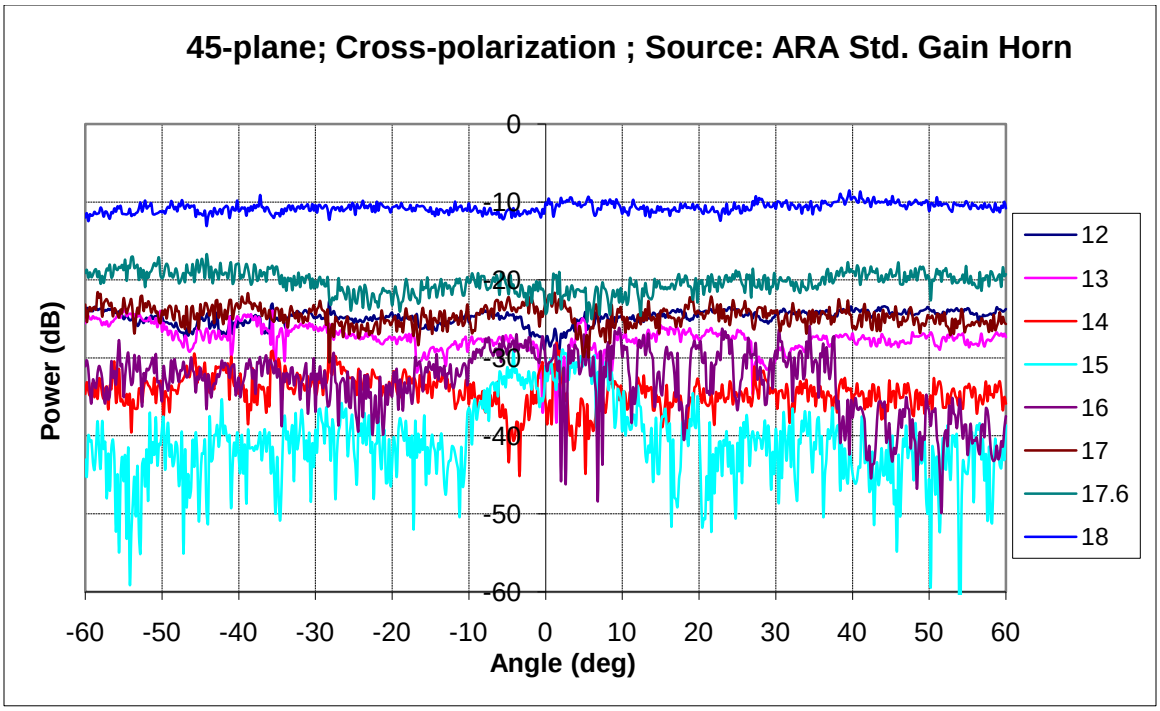

Figure 5. Measured (OATR) Cross-polarized Patterns; 45˚-plane

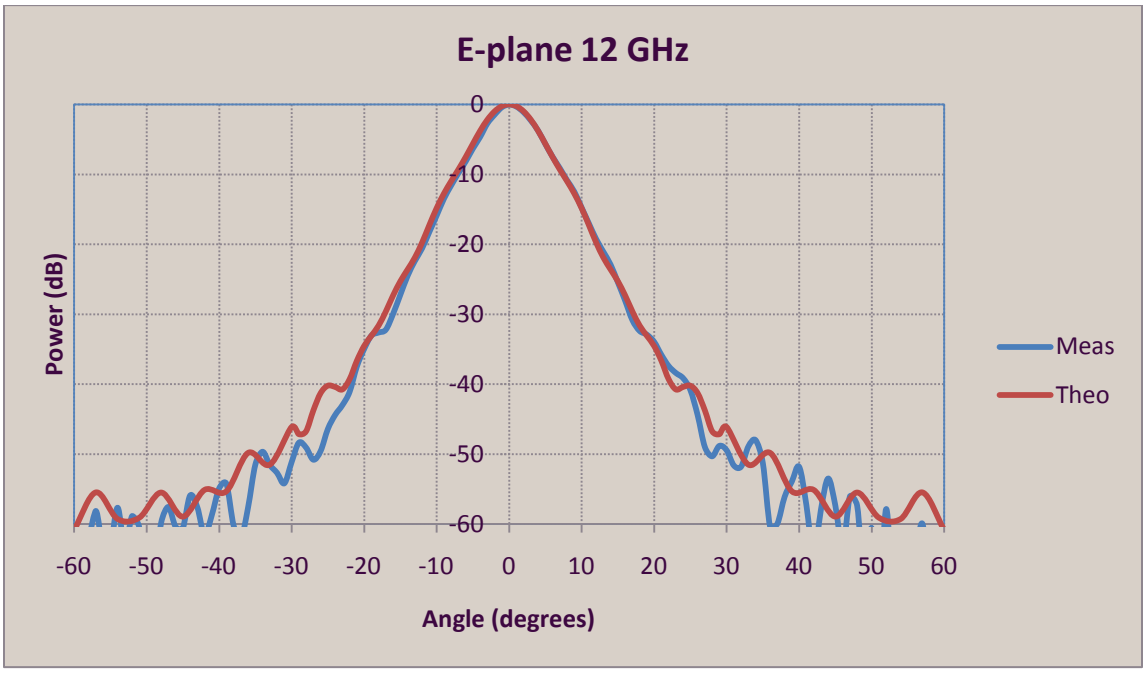

Figure 6. Measured (OAR) and Theoretical Patterns at 12 GHz; E-plane

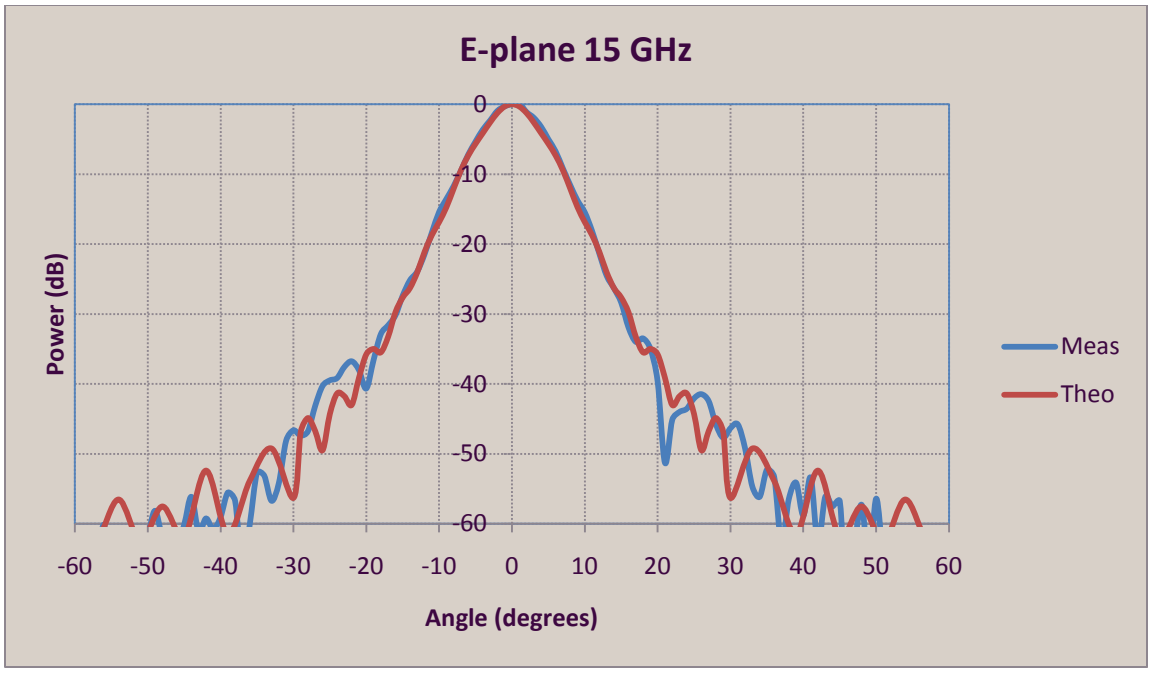

Figure 7. Measured (OAR) and Theoretical Patterns at 15 GHz; E-plane

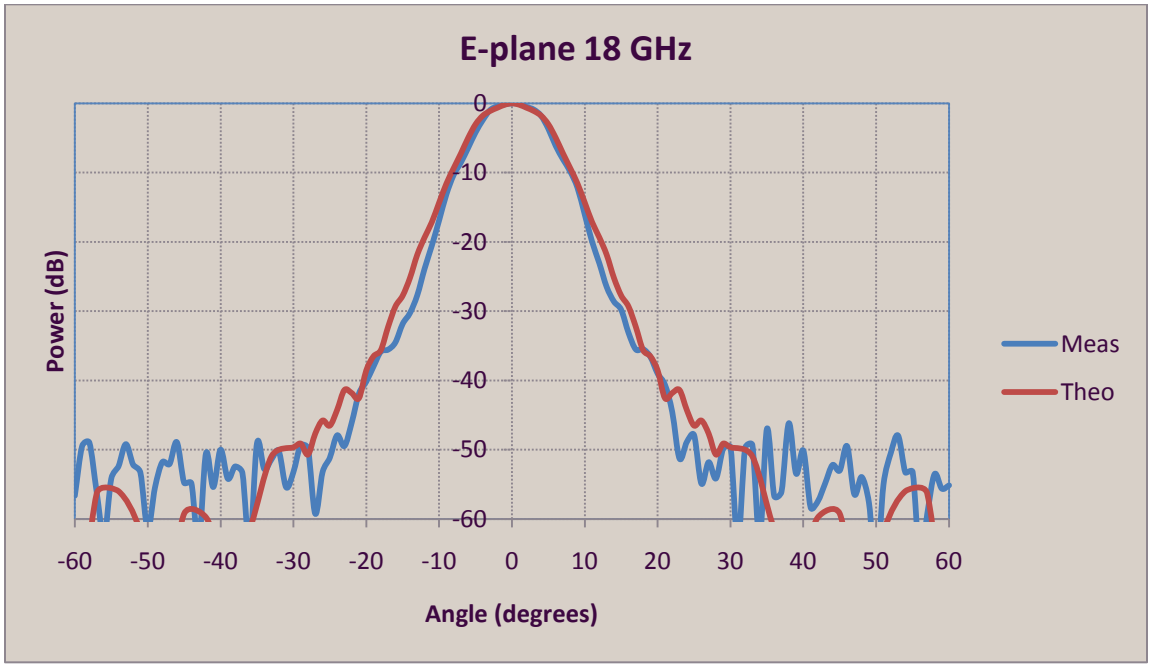

Figure 8. Measured (OAR) and Theoretical Patterns at 18 GHz; E-plane

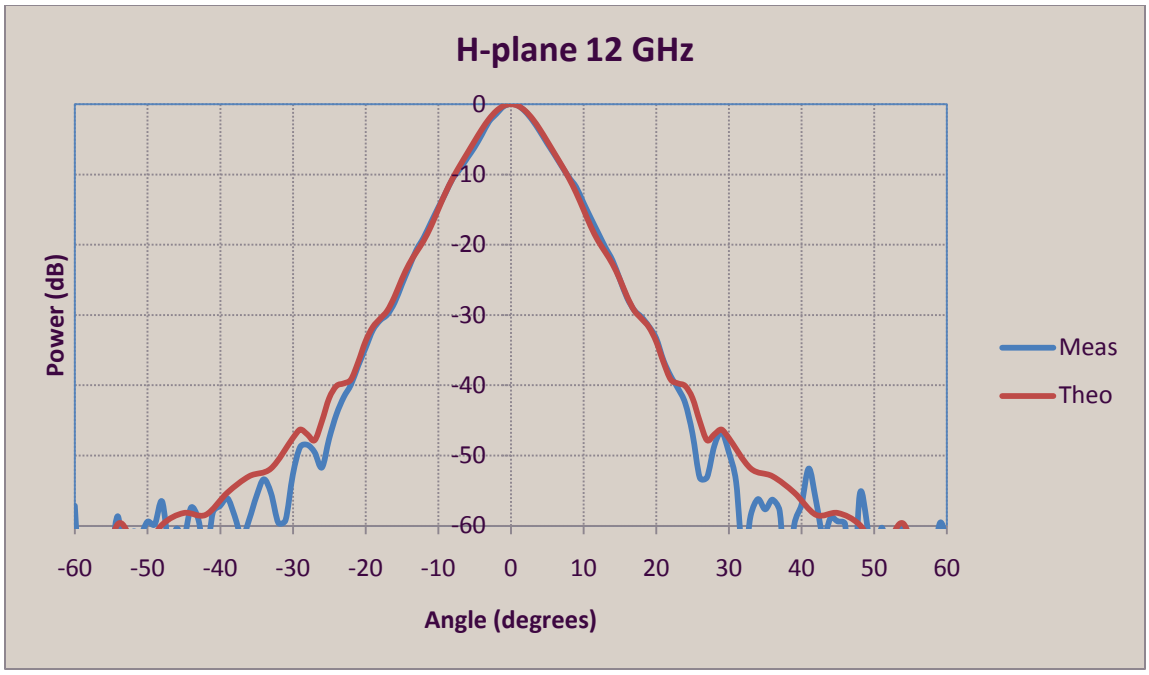

Figure 9. Measured (OAR) and Theoretical Patterns at 12 GHz; H-plane

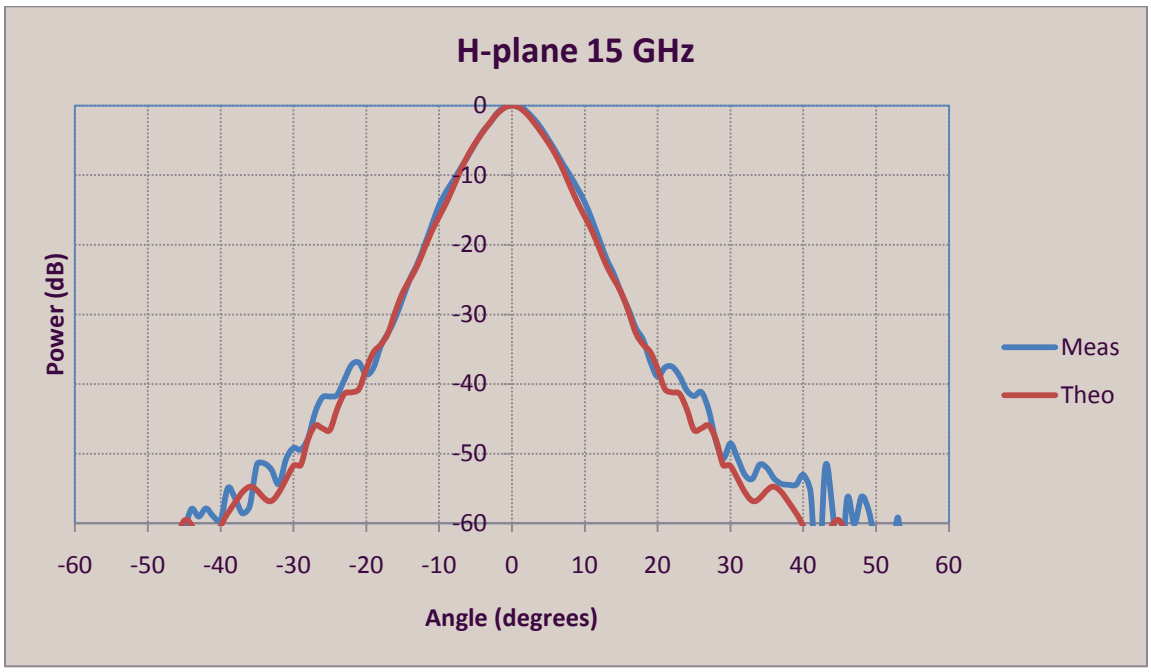

Figure 10. Measured (OAR) and Theoretical Patterns at 15 GHz; H-plane

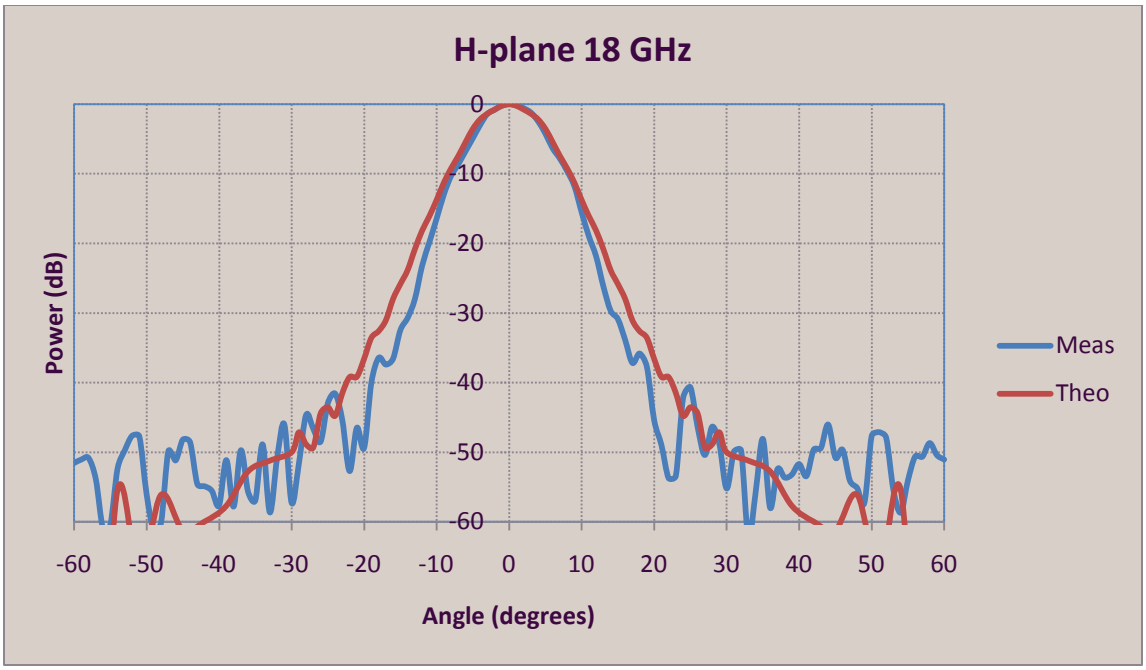

Figure 11. Measured (OAR) and Theoretical Patterns at 18 GHz; H-plane

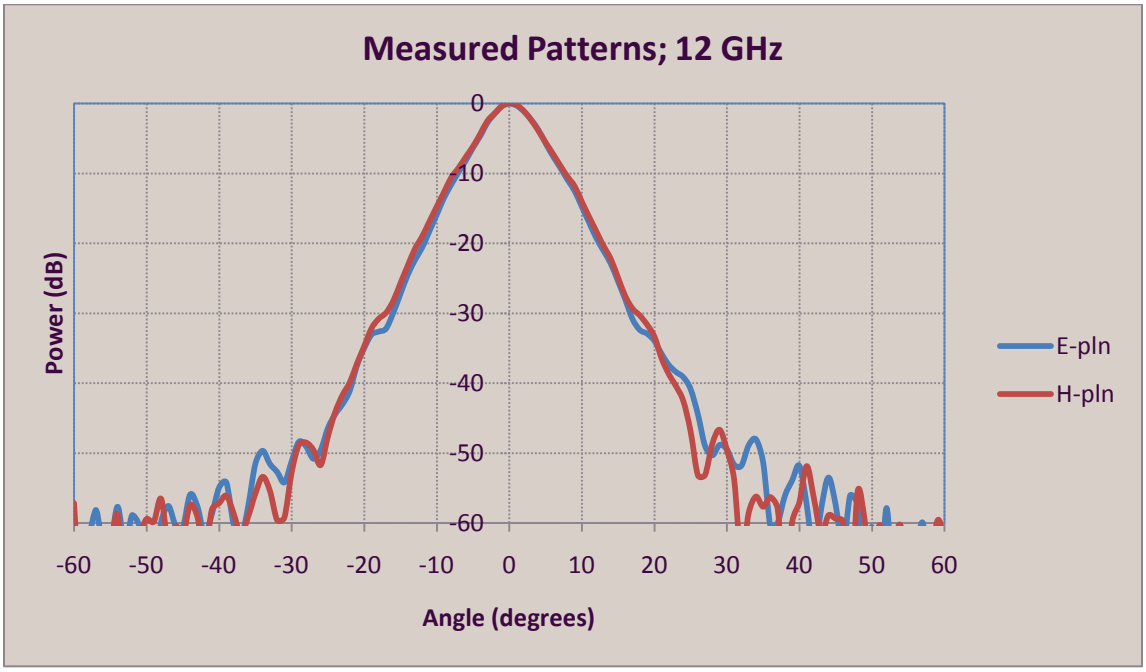

Figure 12. Measured (OAR) Patterns at 12 GHz; E-, H-planes

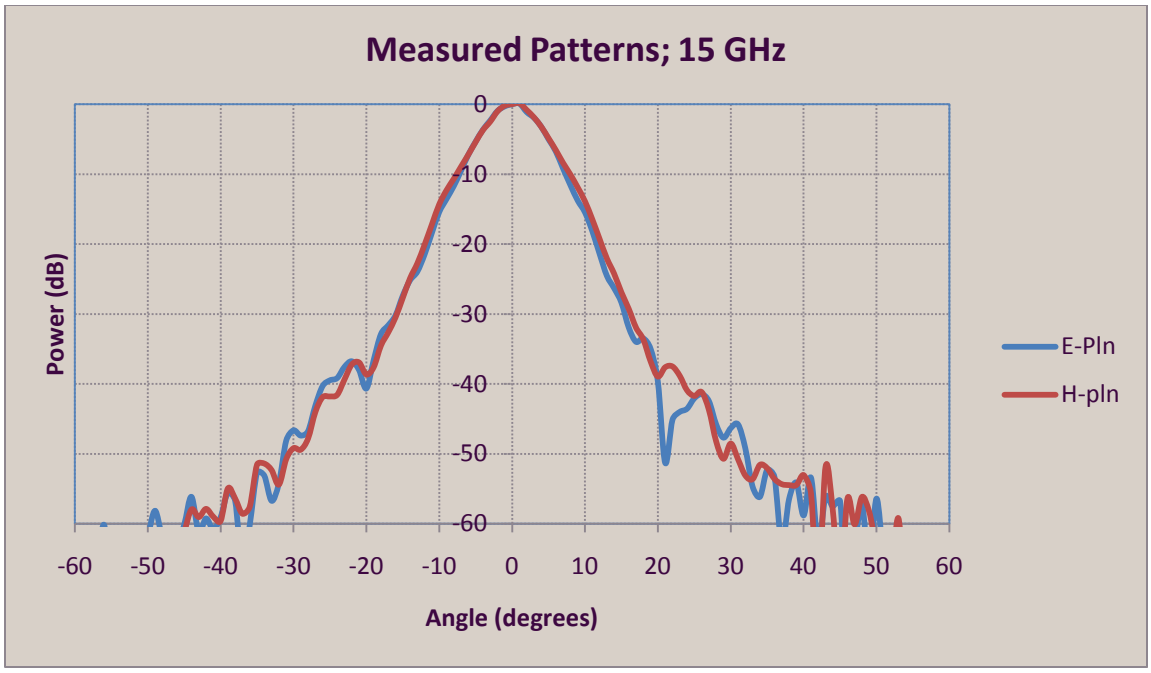

Figure 13. Measured (OAR) Patterns at 15 GHz; E-, H-planes

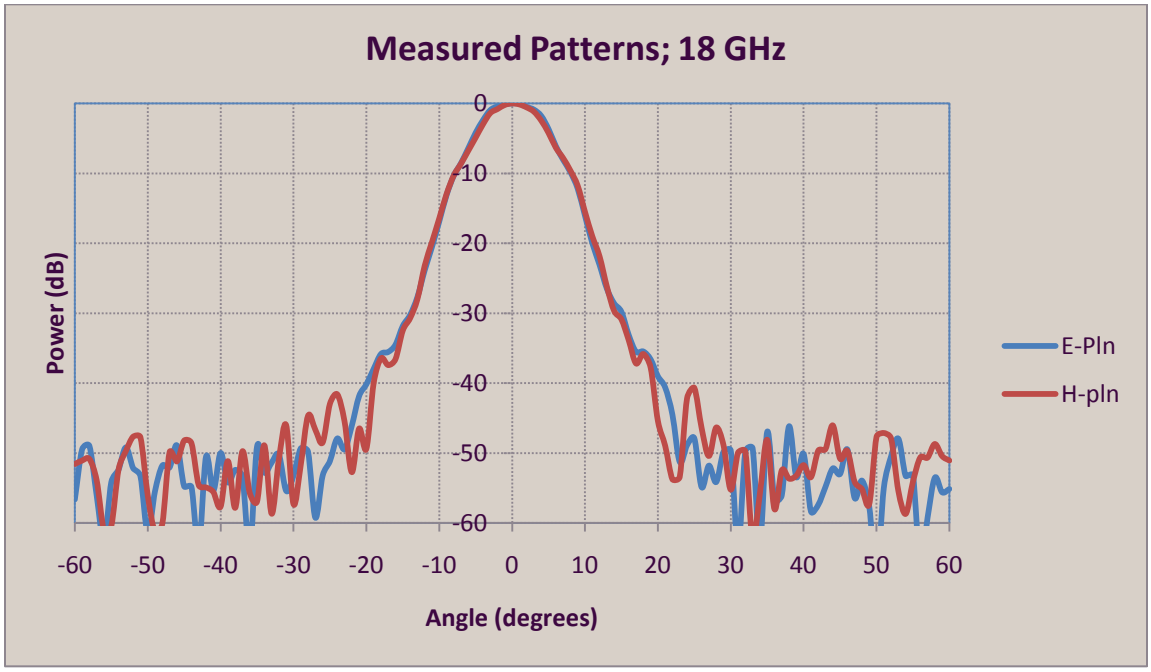

Figure 14. Measured (OAR) Patterns at 18 GHz; E-, H-planes

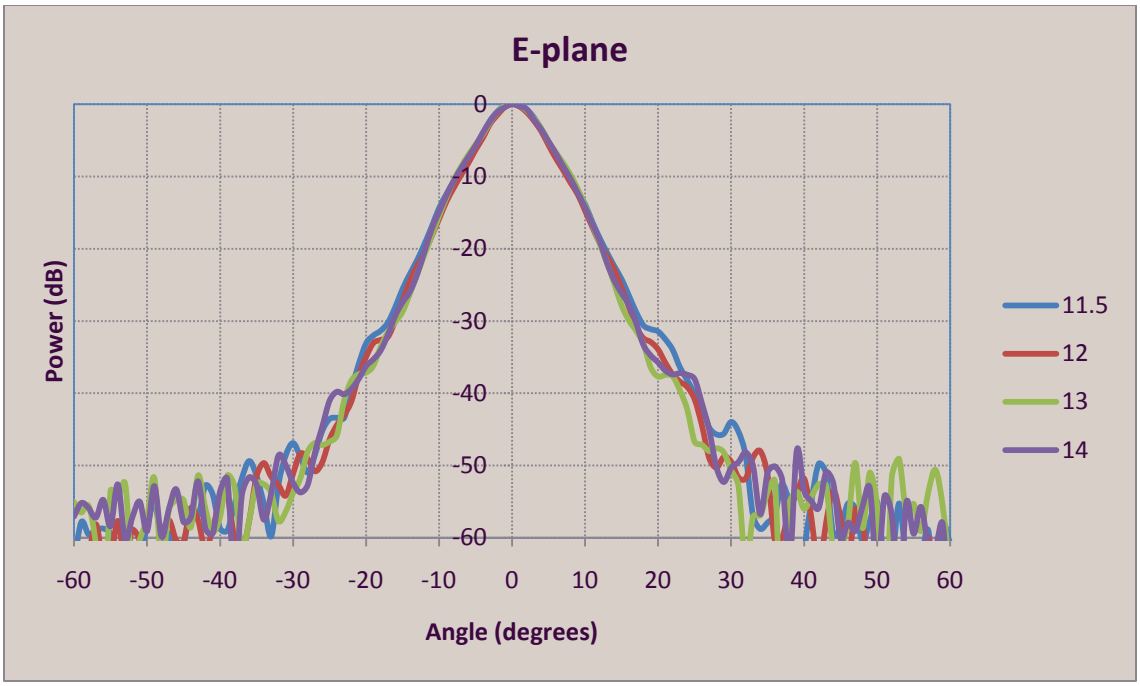

Figure 15a. Measured (OAR) Patterns in E-plane 11.5-14 GHz

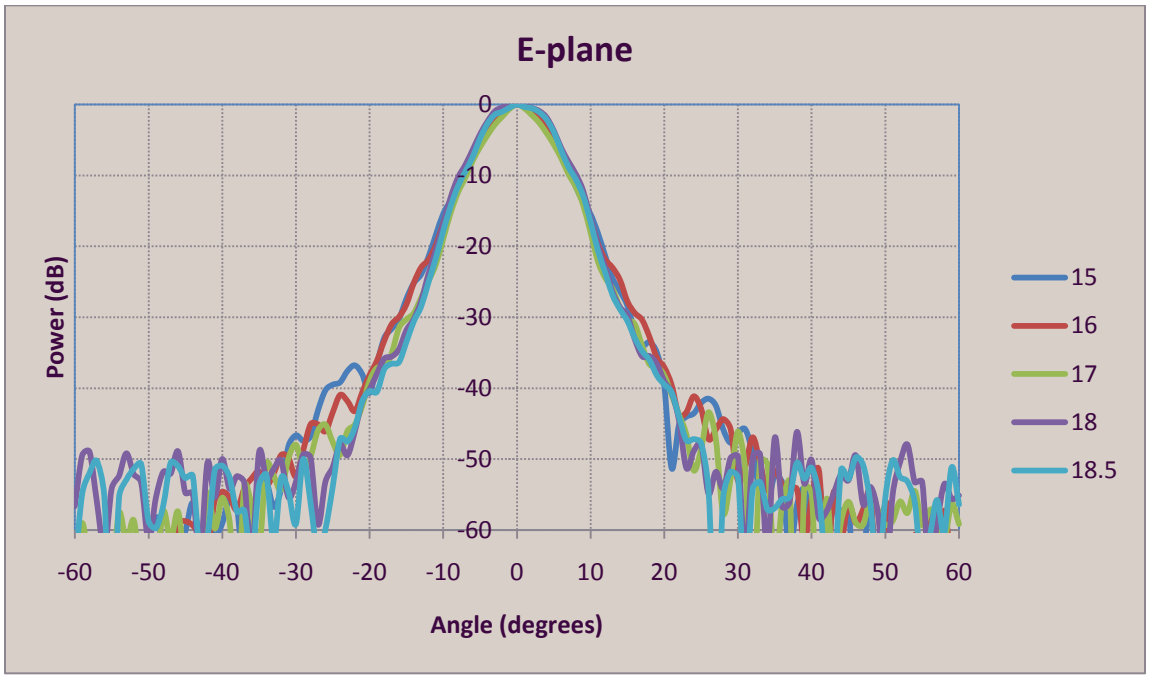

Figure 15b. Measured (OAR) Patterns in E-plane 15-18.5 GHz

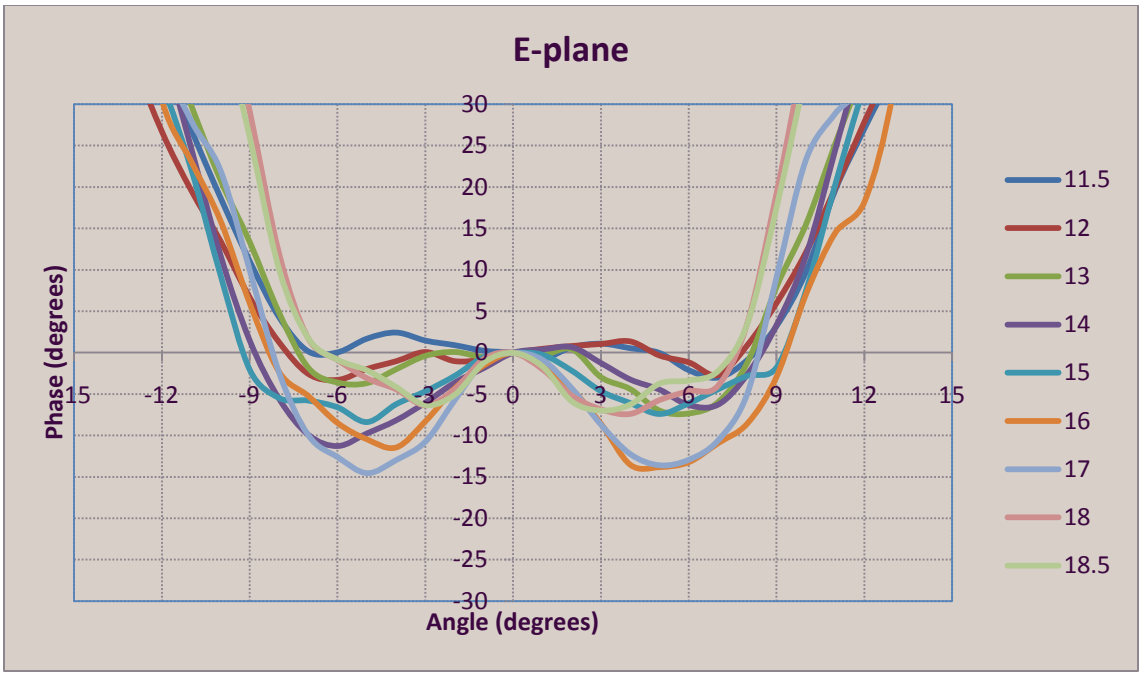

Figure 16. Measured (OAR) Phase Patterns in E-plane

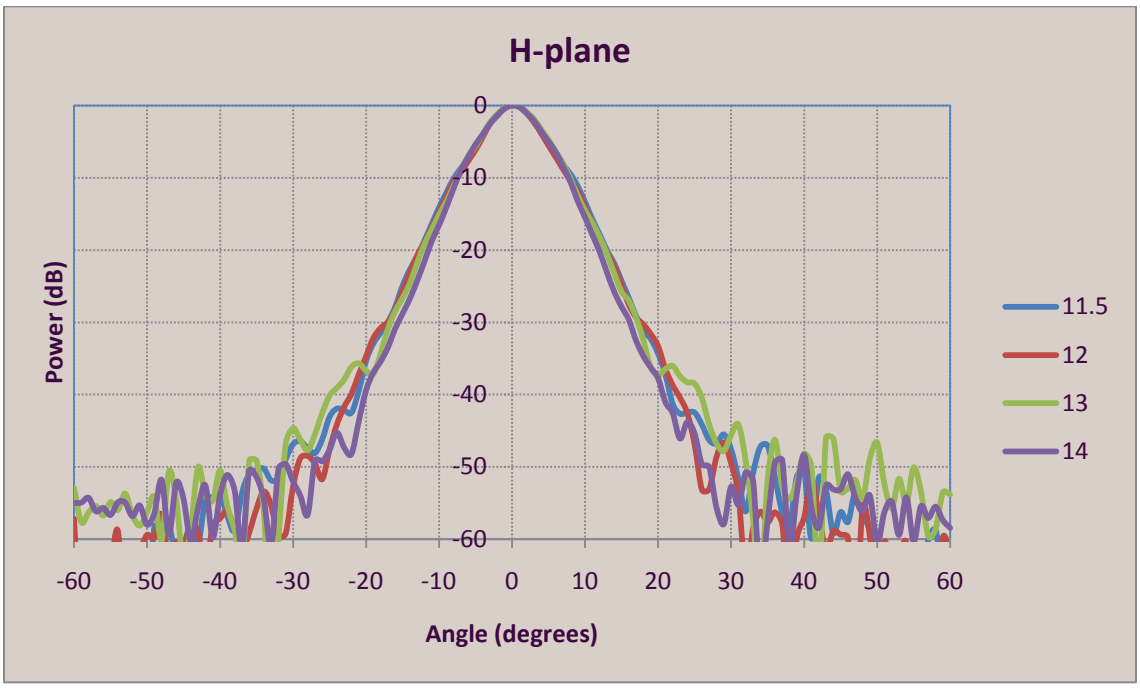

Figure 17a. Measured (OAR) Patterns in H-plane 11.5-14 GHz

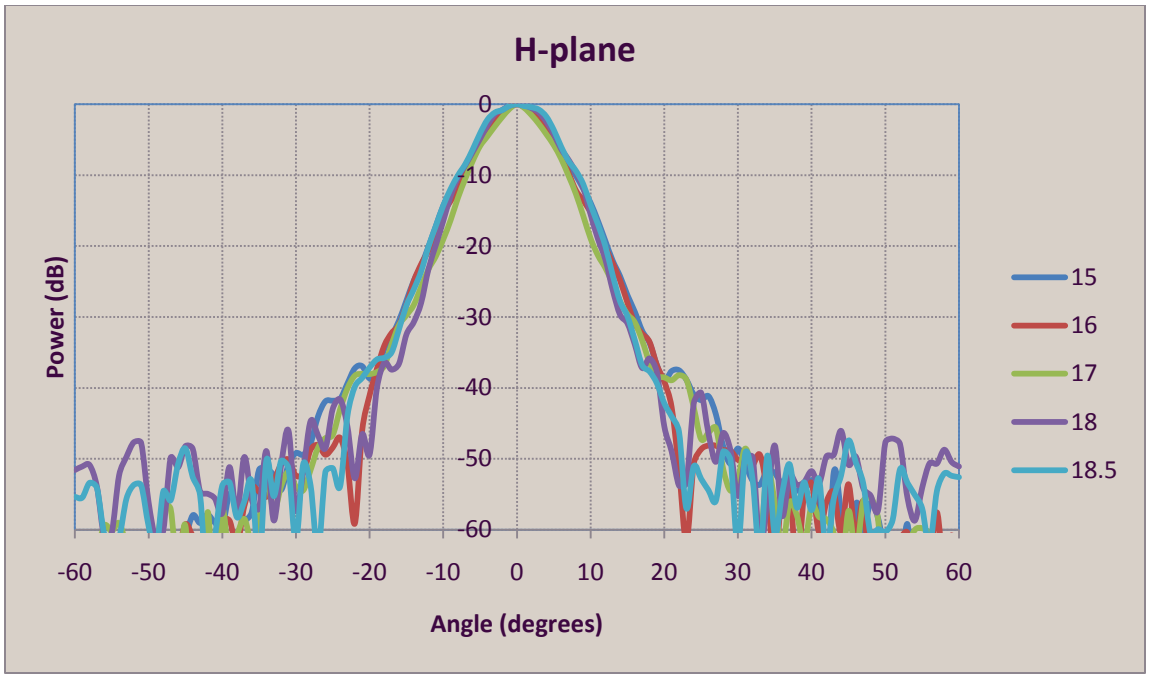

Figure 17b. Measured (OAR) Patterns in H-plane 15-18.5 GHz

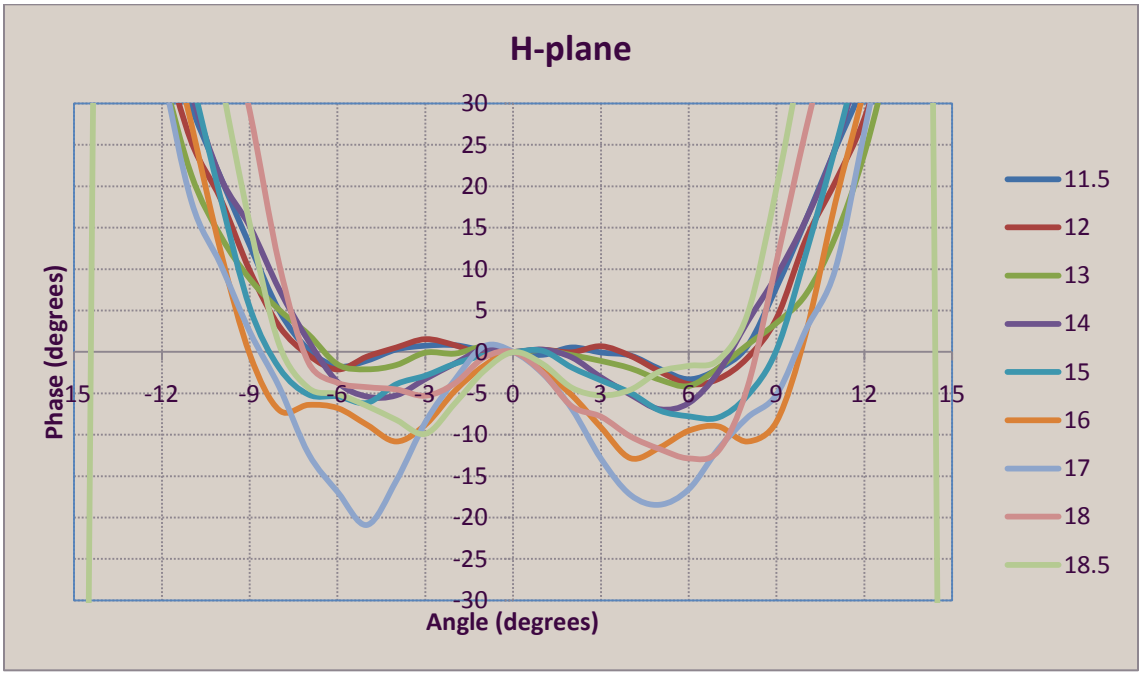

Figure 18. Measured (OAR) Phase Patterns in H-plane

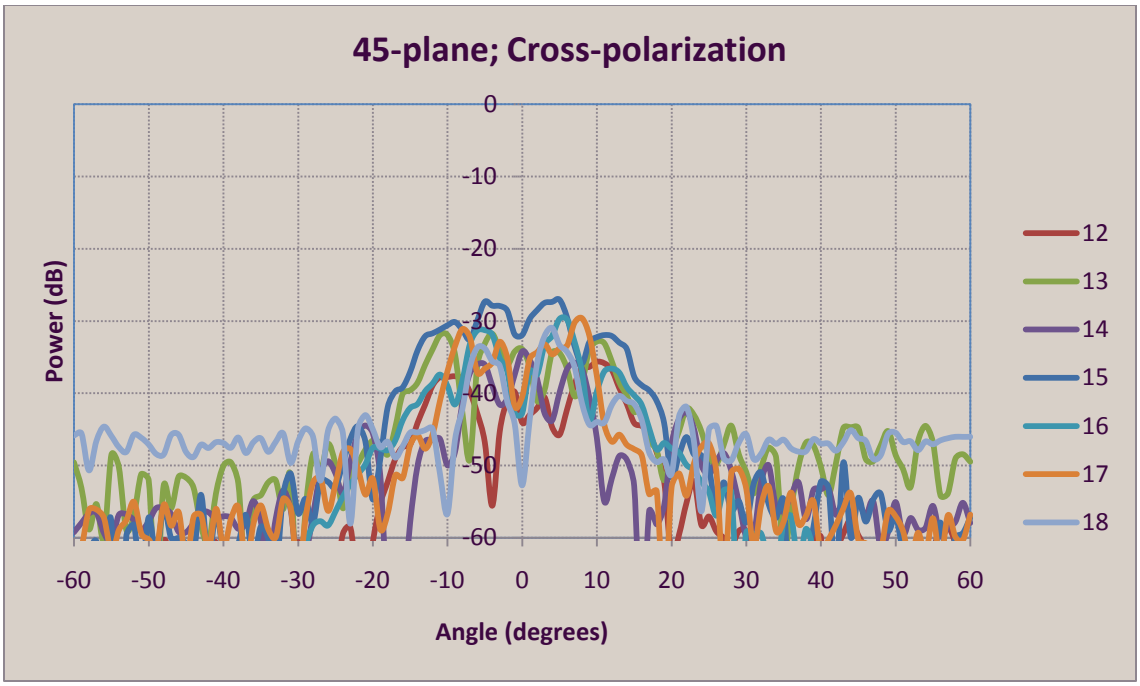

Figure 19. Measured (OAR) Cross-polarized Patterns; 45°-plane

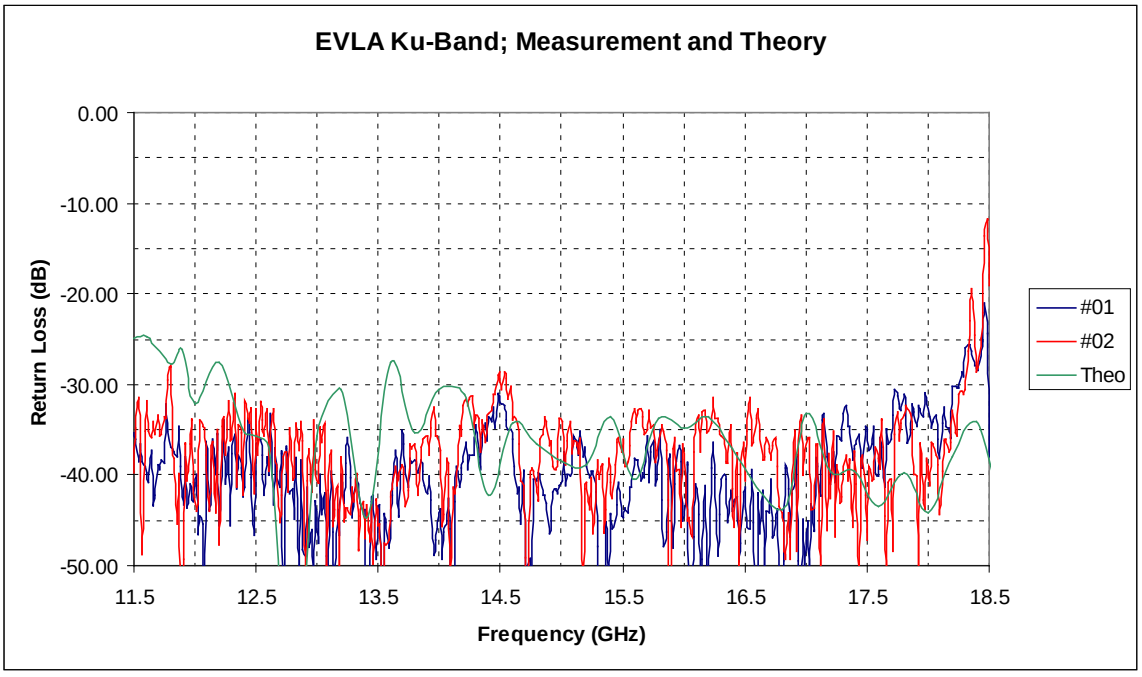

Figure 20. Return Loss of Feeds Horns #1 & #2; Measured and Theory